The Ricean K Factor: Estimation and Performance Analysis

C. Tepedelenlioğlu,
Contact Author
Arizona State University
Telecommunication Research Center
cihan@asu.edu
Tel: (480) 965-6623

A. Abdi,
New Jersey Institute of Technology
Dept. of Elect. and Comp. Engr.
ali.abdi@njit.edu
Tel: (973) 596-5621

G. B. Giannakis
University of Minnesota
Dept. of Elect. and Comp. Engr.
georgios@ece.umn.edu
Tel: (612) 626-7781

Suggested Associate Editorial Areas:
- Detection and estimation
- Propagation and channel characterization

Abstract

In wireless communications, the relative strength of the direct and scattered components of the received signal, as expressed by the Ricean K factor, provides an indication of link quality. Accordingly, efficient and accurate methods for estimating K are of considerable interest. In this paper, we propose a general class of moment-based estimators which use the signal envelope. This class of estimators unifies many of the previous estimators, and introduces new ones. We derive, for the first time, the asymptotic variance of these estimators and compare with the Cramer-Rao bound (CRB). We then tackle the problem of estimating K from the in-phase and quadrature-phase (I/Q) components of the received signal, and illustrate the improvement in performance, as compared to the envelope-based estimators. We derive the CRBs for the I/Q data model, which, unlike the envelope CRB, is tractable for correlated samples. Furthermore, we introduce a novel estimator that relies on the I/Q components, and derive its asymptotic variance even when the channel samples are correlated. We corroborate our analytical findings by simulations.

Original version was submitted to the *IEEE Transactions on Wireless Communications* Dec. 24, 2001, revised August 23, 2002. Parts of this work have been presented [24] and [25]. This work has been supported by the National Science Foundation, through the Career grant No. CCR-0133841 (first author), and the Wireless Initiative Program, Grant No. 9970443 (third author).

I. Introduction and Signal Model

In wireless communications, when there is a line of sight (LoS) between the transmitter and the receiver, the received signal can be written as the sum of a complex exponential and a narrowband Gaussian process, which are known as the 'LoS component' and the 'diffuse component', respectively. The ratio of the powers of the LoS component to the diffuse component is the Ricean factor, which measures the relative strength of the LoS, and hence is a measure of link quality. Consider the communication scenario in Fig. 1 where an unmodulated carrier is transmitted, and the receiver that is traveling with a velocity v receives the transmitted waveform through a LoS component and many multipath components. The baseband in-phase/quadrature-phase (I/Q) representation of the received signal can be expressed as:

$$x(t) = \underbrace{\sqrt{\frac{K\Omega}{K+1}}}_{A:=} e^{j(2\pi f_D \cos(\theta_0)t + \phi_0)} + \underbrace{\sqrt{\frac{\Omega}{K+1}}}_{\sigma:=} h(t) \ , \tag{1}$$

where K is the Ricean factor, θ_0 and ϕ_0 are the angle of arrival (AoA) and phase of the LoS respectively, and are assumed to be deterministic parameters; the maximum Doppler frequency f_D is the ratio of the mobile velocity v and the wavelength; $h(t)$ is the diffuse component given by the sum of a large number of multipath components, constituting a complex Gaussian process; the correlation function of $h(t)$ can be expressed as (see e.g., [19])

$$r_h(\tau) := E[h(t)h^*(t+\tau)] = \int_{-\pi}^{\pi} p_h(\theta)\, e^{j2\pi f_D \cos(\theta)\tau} d\theta \ , \tag{2}$$

where $E[\cdot]$ denotes expectation, * denotes conjugation, $p_h(\theta)$ is the AoA distribution of the diffuse component, which, when uniform, yields the well-known Clarke-Jakes correlation function that is expressed in terms of the zeroth order Bessel function of the first kind: $r_h(\tau) = J_0(2\pi f_D \tau)$ [19]. Without loss of generality, we are assuming $E|h(t)|^2 = 1$ which implies that the power of the diffuse component in (1) is σ^2. Similarly, the power of the LoS component is given by A^2. Notice that A and σ in (1) are defined in such a way that the ratio A^2/σ^2 yields the Ricean K factor, and the received signal power is given by $E|x(t)|^2 = A^2 + \sigma^2 = \Omega$. In fact, it is often the envelope $R(t) := |x(t)|$ that is of interest, and its marginal probability density function (pdf) can be expressed in terms of Ω and K as (see e.g., [19])

$$p_R(r) = \frac{2(K+1)r}{\Omega} \exp\left(-K - \frac{(K+1)r^2}{\Omega}\right) I_0\left(2r\sqrt{\frac{K(K+1)}{\Omega}}\right) \ , \tag{3}$$

where $I_n(\cdot)$ is the n^{th} order modified Bessel function of the first kind. Notice that when $K = 0$, there is no LoS component, in which case (3) reduces to the Rayleigh distribution.

The relative power of the LoS component, represented by the K factor, is a useful measure of the communication link quality. Therefore, estimation of K is important in a variety of wireless scenarios, including channel characterization, link budget calculations, adaptive modulation, and geolocation applications [8], [12]. Moreover, recent advances in space-time coding have shown that the capacity and performance of multiple input multiple output (MIMO) systems depend on the Ricean factor [22]. This has lead [3] to consider adaptive modulation schemes for MIMO systems where the adaptation is based on the Ricean factor rather than the instantenous channel coefficients. Hence, estimation of the Ricean factor is important not only for channel characterization, but also in adaptive modulation schemes where accurate estimates and the knowledge of the estimation error is crucial for proper system operation.

Estimation of the Ricean factor has been tackled in quite disparate contexts. In [15], Rastogi and Holt propose a moment-based approach which utilizes the second and fourth order moments of the envelope $R(t)$, in order to estimate K from the HF radio waves (see also [9]). In [21], the maximum likelihood estimator (MLE) is derived, and is shown to require a cumbersome inversion of a nonlinear function of K. In the same reference, a simpler estimator that utilizes the first and second order moments of the received envelope, which also requires the inversion of a nonlinear function of K is proposed (this estimator was later rediscovered in [14]). In [1], two moment-based estimators are compared using asymptotic analysis and simulations. The distribution fitting approaches for estimating K, proposed in [8], are robust, but are not suited for online implementation due to their complexity and hence might be more useful for *testing* whether the measured envelope is Ricean distributed, rather than estimating K. An expectation-maximization approach to finding the MLE for a multidimensional Ricean distribution is proposed in [11], but still not easy to calculate and use in a communication scenario. In [7], the moment-based approach that uses the second and fourth moments of the envelope (originally mentioned in [15]) is derived from a different perspective, assuming the LoS component in (1) is time-invariant. A dynamic approach based on the received uncoded bit error rate (BER) is recently proposed in [20].

In most of these references, the received data is assumed to be independent and identically distributed (iid). Neither the effect of correlation nor the influence of the LoS AoA θ_0 on the performance has been addressed in the literature. Performance analysis of the aforementioned estimators have mainly relied on simulations. In addition, mostly estimation from the envelope $R(t)$ has been investigated, and a general framework for moment-based estimators has not been derived. Moreover, the potential performance improvements attainable by using the I/Q components rather than the envelope have not been fully addressed. We will fill these gaps in this paper. More specifically,

we propose a general family of moment-based estimators that rely on the envelope $R(t)$, which includes the moment-based estimators in [7], [14], [15], and [21], as special cases. The asymptotic performance analysis of these moment-based estimators are performed for the first time and compared to the Cramer-Rao bound (CRB). In addition we investigate, for the first time, the estimation of K from the I/Q components of the flat fading channel coefficient given in complex baseband form by (1). The I/Q components of the channel (or their estimates) are available in applications where a coherent estimate of the channel is necessary. We show that using the I/Q components (which contain phase information of the channel) improves the estimator performance, especially for small values of K. Moreover, we will see that, unlike the estimators that utilize the envelope, the performance analysis of the estimators that utilize the I/Q components and the corresponding CRB can be computed even when the samples of $x(t)$ are *correlated*. We will derive the rate of convergence of the estimators that utilize the I/Q components, which will require a novel approach because the samples of (2) are not absolutely summable.

The paper is organized as follows. In Section II we propose a general class of moment-based estimators for K that use the envelope $R(t)$, derive the asymptotic variance, and compare it with the CRB, derived under the iid assumption. In Section III we derive the CRB for the I/Q data, allowing for possible correlation and observe that there might be significant gains in performance if the I/Q components are utilized. This motivates us to derive an FFT-based estimator and its asymptotic performance, which is shown to be better than the envelope-based estimators. In Section IV we corroborate our analytical results with computer simulations, and Section V concludes the paper.

II. Moment-Based Estimation of K from the Envelope

The moments of the Ricean distribution, expressed in terms of σ^2 and K, are given by [19]:

$$\mu_n := E[R^n(t)] = (\sigma^2)^{n/2}\ \Gamma\left(n/2+1\right)\ \exp(-K)\ {}_1F_1\left(n/2+1;1;K\right)\ , \tag{4}$$

where ${}_1F_1(\cdot;\cdot;\cdot)$ is the confluent hypergeometric function, and $\Gamma(\cdot)$ is the gamma function. We see from (4) that the moments depend on the two unknown parameters K and σ. Hence, a moment-based K estimator requires estimates of at least two different moments of $R(t)$. More specifically, suppose that for $n \neq m$ we define the following functions of K (recall that μ_n is the n^{th} moment of $R(t)$):

$$f_{n,m}(K) := \frac{\mu_n^m}{\mu_m^n}\ . \tag{5}$$

Since by (4) and (5), $f_{n,m}(K)$ depends only on K and not on σ, we can construct moment-based estimators for K by using sample moments instead of the ensemble values in (5) and then inverting

the corresponding $f_{n,m}(K)$, to solve for K. Hence, an estimator that depends on the m^{th} and n^{th} moments could be expressed as:

$$\hat{K}_{n,m} := f_{n,m}^{-1}\left(\frac{\hat{\mu}_n^m}{\hat{\mu}_m^n}\right) \quad \text{with} \;\; \hat{\mu}_k := \frac{1}{N}\sum_{l=0}^{N-1} R^k(lT_s)\;, \tag{6}$$

where N is the number of available samples, T_s is the sampling period, and we assume that the inverse function $f_{n,m}^{-1}(\cdot)$ exists. For all the values of m and n we considered, $f_{n,m}(K)$ is a monotone increasing function in the interval $K \in (0,\infty)$, and hence the inverse function $f_{n,m}^{-1}(\cdot)$ does exist. Notice that the moment estimator $\hat{\mu}_k$ can be updated using a sliding window of length N, which would be useful in real-time estimation of K.

The natural choice for (n,m) is $(1,2)$ since this selection involves the lowest order moments. When $n=1$ and $m=2$, (5) can be calculated using (4) as:

$$f_{1,2}(K) = \frac{\pi e^{-K}}{4(K+1)}\left[(K+1)I_0\left(\frac{K}{2}\right) + KI_1\left(\frac{K}{2}\right)\right]^2 \;. \tag{7}$$

The corresponding estimator $\hat{K}_{1,2}$ involves the complex numerical procedure of inverting (7). This estimator has been discussed in [14] and its performance was studied in [21] via simulations where it was found that $\hat{K}_{1,2}$ performs similarly to the MLE. The MLE is given as the value of K that satisfies the following equation [21]:

$$\frac{1}{1+K} + \frac{(1+2K)}{N\sqrt{K(K+1)}}\sum_{l=0}^{N-1} R(lT_s)\,\frac{I_1\left(2R(lT_s)\sqrt{K^2+K}\right)}{I_0\left(2R(lT_s)\sqrt{K^2+K}\right)} = 1+\hat{\mu}_2 \tag{8}$$

which is evidently even more difficult to compute than $\hat{K}_{1,2}$, because (7) can be inverted using a lookup table, but this is not possible when the value of K that satisfies (8) is sought for the MLE. This is because one cannot rearrange (8) to have a function of K that does not depend on $R(t)$ on one side of the equation, and something that only depends on the data $R(t)$ (and not on K) on the other side. So the MLE requires an exhaustive search, or a root-finding technique such as Newton's method where the convergence of the root estimate depend on $R(lT_s)$ and might not always be guaranteed.

A simpler alternative to $\hat{K}_{1,2}$ is $\hat{K}_{2,4}$. It can be shown using (4) and (5) that

$$f_{2,4}(K) = \left[\frac{(K+1)^2}{K^2+4K+2}\right]^2 \;. \tag{9}$$

Solving for $\hat{K}_{2,4}$ from an estimate of the left hand side in (9) involves finding the roots of a second-order polynomial which can be done in closed form. It can be shown that one of the roots of this

polynomial is always negative which can be discarded since $K \geq 0$, yielding a unique non-negative solution for $\hat{K}_{2,4}$ which is given by:

$$\hat{K}_{2,4} = \frac{-2\hat{\mu}_2^2 + \hat{\mu}_4 - \hat{\mu}_2\sqrt{2\hat{\mu}_2^2 - \hat{\mu}_4}}{\hat{\mu}_2^2 - \hat{\mu}_4} \ . \tag{10}$$

The estimator in (10) has been known since [9, 15] in the context of HF channel modeling, and recently re-emerged in the wireless communications literature in [7], though not presented in this general setting. In what follows, we derive novel asymptotic variance (AsV) expressions for $\hat{K}_{n,m}$, where n and m are arbitrary moment orders.

A. Asymptotic Variance of Moment-Based Estimators

In order to derive the AsV of the estimators proposed in this paper, we will be using the following well-known result which is obtained by slightly adapting [13, Theorem 3.16] to our problem.

Theorem: *Suppose the two statistics $X_1(N)$ and $X_2(N)$ converge to x_1 and x_2 respectively in the mean squared sense, and the estimator of interest is given as a function of these statistics: $\hat{K}(N) = g(X_1(N), X_2(N))$. Let $d(N)$ denote the rate of convergence of the vector $[X_1(N)X_2(N)]$, so that $d(N)[(X_1(N) - x_1) \ \ (X_2(N) - x_2)]$ converges to a random vector with mean zero, and covariance matrix whose (l, k) element is given by*

$$c_{lk} := \lim_{N\to\infty} d^2(N)\mathrm{cov}(X_l(N), X_k(N)) \ , \quad l, k = 1, 2 \ . \tag{11}$$

Then the scaled estimator $d(N)(g(X_1(N), X_2(N)) - g(x_1, x_2))$ converges in distribution to a random variable with zero mean and variance given by

$$\mathrm{AsV} = \sum_{l=1}^{2}\sum_{k=1}^{2} c_{lk}\frac{\partial g(a_1, a_2)}{\partial a_l}\frac{\partial g(a_1, a_2)}{\partial a_k}\Big|_{a_1=x_1, a_2=x_2} \ . \tag{12}$$

We can now use the Theorem to calculate the AsV for the moment-based estimators when the envelope samples are assumed to be iid. In this case, $g(a_1, a_2) = f_{n,m}^{-1}(a_1^m/a_2^n)$, $X_1(N) = \hat{\mu}_n$, $X_2(N) = \hat{\mu}_m$, $x_1 = \mu_n$, $x_2 = \mu_m$, and $d(N) = \sqrt{N}$ (meaning that $X_1(N)$ and $X_2(N)$ are $\sqrt{N}$-consistent because of the iid assumption). Using (12) and the standard result for the derivative of an inverse function, we can express the AsV as follows:

$$\begin{aligned}\mathrm{AsV}(\hat{K}_{n,m}) = \left(\frac{m\mu_m^{-n}\mu_n^{m-1}}{f'_{n,m}(K)}\right)^2(\mu_{2n} - \mu_n^2) - 2\frac{m\mu_m^{-n}\mu_n^{m-1}}{f'_{n,m}(K)}\frac{n\mu_m^{-n-1}\mu_n^m}{f'_{n,m}(K)}(\mu_{n+m} - \mu_n\mu_m) \\ + \left(\frac{n\mu_m^{-n-1}\mu_n^m}{f'_{n,m}(K)}\right)^2(\mu_{2m} - \mu_m^2) \ ,\end{aligned} \tag{13}$$

where $f'_{n,m}(K)$ is the derivative of $f_{n,m}(K)$ with respect to K, and can be computed using (4) and (5). Hence we can conclude that all moment-based K estimators, $\hat{K}_{n,m}$ in (6), are $\sqrt{N}$-consistent, and asymptotically unbiased, with asymptotic variance given by (13). Notice that (13) is a function of only (K, n, m) and does not depend on Ω. This can easily be seen from the fact that the estimator in (6) is scale invariant (i.e., if the envelope data is multiplied by a constant, the estimator in (6) remains the same).

In order to compare the AsV expression in (13) with a benchmark, we numerically computed the CRB, which provides a lower bound for the variance of any unbiased estimator. The CRB was reported in [21] as

$$\mathrm{CRB}(K) = \left[N \int_0^\infty \left(\frac{\partial}{\partial K} [\ln p_R(r)] \right)^2 p_R(r) dr \right]^{-1}, \tag{14}$$

but this expression assumes that the only unknown is K, and that $\Omega = E|x(t)|^2$ is known. The CRB for the more realistic scenario that Ω is unknown can be derived from the Fischer Information Matrix (FIM) of $[K\ \Omega]$, by using the (1,1) element of the inverse FIM, and is shown to be greater than the CRB for the known Ω, which is a well-known consequence of Ω being a nuisance parameter [10]. We show in Appendix I, how this is done numerically. It is important to point out that whether Ω is known or not, affects the CRB. However the *value* of Ω does not affect the CRB, because the CRB is scale invariant, and hence does not depend on the second moment Ω.

Fig. 2 plots the asymptotic standard deviation (square root of the AsV) for $\hat{K}_{1,2}$, $\hat{K}_{1,3}$, and $\hat{K}_{2,4}$, as well as the square root of the CRB for known and unknown Ω, which collectively illustrate the performance of moment-based estimators for large sample sizes. As expected, the CRB for known Ω is smaller than the CRB for unknown Ω, even though the difference is very small. In the rest of this section, unless otherwise noted, CRB will refer to the realistic case where Ω is unknown. Notice from Fig. 2 that as K gets smaller, making the Ricean pdf more like Rayleigh, no unbiased envelope-based estimator can estimate K accurately, because the CRB goes to infinity. We also observe that the most accurate estimation of K from the envelope $R(t)$ is possible around $K = 1$. Note also that as K increases, the asymptotic standard deviation goes to infinity approximately linearly. Among the moment-based estimators, $\hat{K}_{1,2}$ (dashed line) has the least AsV for moderate/large K, and is in fact indistinguishable from the CRB for $K > 1.5$, which leads us to conclude that $\hat{K}_{1,2}$ is *almost* asymptotically efficient. As we expected, increasing m and n (implying usage of higher-order moments) result in larger AsV for moderate/large K. Indeed, the simple estimator $\hat{K}_{2,4}$ in (10), for which there is a closed form expression, and $\hat{K}_{1,3}$ have a greater AsV than that of $\hat{K}_{1,2}$.

After we have introduced and analyzed the family of estimators $\hat{K}_{n,m}$ that utilize the envelope

samples, we notice that two of these estimators are noteworthy: $\hat{K}_{1,2}$ has the best asymptotic performance of all the moment-based estimators with integer moments, which is indistinguishable from the CRB, and $\hat{K}_{2,4}$ in (10) has a simple closed-form solution which is easier to implement in practice.

III. Estimation of K from the I/Q Components

In this section, we will investigate the estimation of K from the I/Q components of the received signal given in complex baseband form, which are the real and imaginary parts of (1). To the best of our knowledge, this is the first estimator of K that uses the I/Q components. The I/Q components are available in applications where a coherent estimate of the channel is necessary. We will show that using the I/Q components (which contain envelope *and* phase information of the channel) improves the estimator performance, especially for small values of K.

A. CRB for I/Q Data

In this section we will derive the CRB for the variance of K estimators that use the I/Q data in (1). The resulting CRB will be a lower bound on the variance of any unbiased estimator for K obtained not only from the I/Q components in (1), but also from the envelope. This is because any estimator that can be constructed from the envelope can be constructed from (1). We will see that unlike the derivation of the envelope CRB, we will not need to make the restrictive iid assumption when deriving the I/Q CRB because of the tractability of the multivariate Gaussian pdf (as opposed to the difficulty of expressing and working with the multivariate Ricean pdf that emerges with correlated envelope samples). CRBs for fading parameters for a differently parameterized radio transmission channel can also be found in [5].

Let us define the T_s-spaced samples of (1) as $x[n] := x(nT_s)$, $\omega_0 := 2\pi f_D \cos(\theta_0) T_s$ and $h[n] := h(nT_s)$. We may then express the sampled I/Q signal in terms of σ and K as follows:

$$x[n] = \sqrt{K}\sigma e^{j(\omega_0 n + \phi_0)} + \sigma h[n] \; . \tag{15}$$

Suppose that we have a data record of N samples from (15). We would like to compute the CRB for the parameter K. We emphasize that the I/Q CRB in this section is different from the envelope CRB, because the data from which they are derived are different. We will calculate the I/Q CRB for two cases:

(i) All the parameters (except K) are known;

(ii) All parameters in $\boldsymbol{\zeta} := [K \; \sigma \; \omega_0 \; \phi_0 \; \omega_D]$ are unknown and the channel correlations are given by $r_h[k] := r_h(kT_s) = J_0(\omega_D k)$, where $\omega_D = 2\pi f_D T_s$.

The first case, which appears rather unrealistic, is important because it provides a lower bound on

any estimator of K whether any other parameter is known or not, and whether the envelope or the I/Q components are used. Another reason for considering case (i) is the resulting simplicity of the bound. We shall consider case (i) first, and then we will address case (ii).

Let $\mathbf{x} := [x[0] \dots x[N-1]]^T$ be a length-N vector that contains the available sampled I/Q components, and $\mathbf{e}(\omega_0, \phi_0) := [\exp(j\omega_0 0 + j\phi_0) \dots \exp(j\omega_0(N-1) + j\phi_0)]^T$. Then the mean and covariance matrix of $\mathbf{x}$ are given by $\mathbf{m}(\boldsymbol{\zeta}) := E[\mathbf{x}] = \sigma\sqrt{K}\mathbf{e}(\omega_0, \phi_0)$, and $\boldsymbol{\Gamma}(\boldsymbol{\zeta}) := E[(\mathbf{x} - \mathbf{m}(\boldsymbol{\zeta}))(\mathbf{x} - \mathbf{m}(\boldsymbol{\zeta}))^H] = \sigma^2\mathbf{R}(\omega_D)$, where $\mathbf{R}(\omega_D)$ denotes the normalized [1] covariance matrix of the I/Q components, and ^{H} denotes Hermittian. When all parameters in $\boldsymbol{\zeta}$ except K are known (case (i)), using (33) in Appendix II, it is easy to show that

$$\mathrm{CRB}_{\mathrm{IQ}}(K) = \frac{2K}{\mathbf{e}^H(\omega_0, \phi_0)\, \mathbf{R}^{-1}(\omega_D)\, \mathbf{e}(\omega_0, \phi_0)}\ , \tag{16}$$

which reduces to the simple $2K/N$ when $x[n]$'s are independent (i.e., when $\mathbf{R}(\omega_D) = \mathbf{I}$).

Some remarks are now in order:

Remark 1: Note that if the correlations satisfy $\sum_k |r_h[k]| < \infty$, then we can use the standard results for the asymptotic forms of Toeplitz matrices (see e.g., [6]) to conclude that the asymptotic CRB defined as $\lim_{N\to\infty} N\mathrm{CRB}_{\mathrm{IQ}}(K)$ converges to $2KS_h(\omega_0)$, for $S_h(\omega_0) \neq 0$, where $S_h(\omega)$ is the spectrum of $h[n]$. The absolute summability of the covariances hold, for example, when $h(t)$ is modeled as an autoregressive process. We see that, in this case, if $S_h(\omega_0)$ is large, the CRB increases. However, the correlation function we have adopted in (2), which is a more accurate correlation model for wireless communications, is not absolutely summable in general, so we cannot easily establish the link between $S_h(\omega)$ and the asymptotic CRB in case (i), as we did when $\sum_k |r_h[k]| < \infty$ holds.

Remark 2: The CRB in (16) considers only K as an unknown parameter, which yields a bound that is smaller than the CRB when other parameters of the model in (15) are unknown. Hence, (16) provides a lower bound to the variance of *any* unbiased estimator of K, regardless of whether it is constructed from the envelope or the I/Q components of the signal, or whether any of the other parameters are known.

Remark 3: Unlike the envelope CRB in Fig. 2, as K gets smaller, the I/Q CRB in (16) goes to zero. This is also the case for the CRB for the more realistic case (ii), where $\boldsymbol{\zeta}$ is unknown, which is derived in Appendix II (see (35)). In Fig. 3, we show the CRB for the envelope data model, CRB for case (i) in (16) where the parameters are known, and the CRB for case (ii) in (35) where the parameters are unknown. We observe in Fig. 3 that CRBs for the I/Q data become smaller as K gets smaller for both cases (i) and (ii), which is also proved in the Appendix II for both cases. This reinforces our intuition that the additional phase information in the I/Q data, which is not present in

[1] so that it has ones on the main diagonal

the envelope data, offers potential improvements in estimator performance, particularly for small K. This insight motivates us to search for estimators of K from the I/Q components. We now propose such an estimator.

B. An Estimator of K from the I/Q components

In pursuit of finding an estimator for K from the I/Q components, the first thing that comes to mind is the MLE constructed from the I/Q data (which is different from (8) constructed from the envelope data). But an MLE from the I/Q data will have to involve joint estimation of $K, \sigma, \omega_0, \phi_0$, and ω_D, which requires a multidimensional search and hence is not practical. An alternative to the MLE is a nonlinear least-squares approach of [18], which was proposed to estimate A, ω_0, σ, and ϕ_0, but not K. In what follows we provide a yet simpler approach.

Let $\hat{\omega}_0 = \text{argmax}_\omega |N^{-1} \sum_{n=0}^{N-1} x[n] e^{-j\omega n}|$. Consider now the following statistics of $x[n]$:

$$X_1(N) \;:=\; \frac{1}{N} \sum_{n=0}^{N-1} x[n] e^{-j\hat{\omega}_0 n} \,, \tag{17}$$

$$X_2(N) \;:=\; \frac{1}{N} \sum_{n=0}^{N-1} |x[n]|^2 = \hat{\mu}_2 \,. \tag{18}$$

Let us assume, for the moment, that $\hat{\omega}_0 \approx \omega_0$. Recalling that $x[n] = Ae^{j(\omega_0 n + \phi_0)} + \sigma h[n]$, and substituting it in (17), we arrive at $X_1(N) = Ae^{j\phi_0} + N^{-1}\sigma \sum_{n=0}^{N-1} h[n] e^{-j\omega_0 n}$. Since as seen from (20), $N^{-1} \sum_{n=0}^{N-1} h[n] e^{-j\omega_0 n}$ goes to zero in the mean-squared sense as N increases, we see that for sufficiently large N, $|X_1(N)|^2 \approx A^2$. On the other hand, $\hat{\mu}_2$ in (18) converges to $\Omega = A^2 + \sigma^2$. This prompts us to propose the following estimator for K that approximates A^2/σ^2:

$$\hat{K}_{\text{IQ}}(N) = \frac{|X_1(N)|^2}{X_2(N) - |X_1(N)|^2} \tag{19}$$

Compared to the estimators that rely on the envelope, the I/Q estimator requires a step to estimate ω_0, which can be accomplished with FFT complexity $\mathcal{O}(N \log N)$. Hence the penalty paid for the performance improvements that the I/Q estimator offers is a slight increase in computational complexity. Similar to the moment-based estimators, the I/Q estimator can benefit from updating $X_1(N)$ and $X_2(N)$ using a sliding window for applications requiring estimates of K in real-time. We will now derive the AsV of (19).

C. Asymptotic Variance of $\hat{K}_{\text{IQ}}(N)$

In this section, we calculate the asymptotic variance of $\hat{K}_{\text{IQ}}(N)$ for the case when the samples $x[n]$ are independent, and also when they are correlated. To simplify the analysis we will assume that

$\hat{\omega}_0 \approx \omega_0$. Hence, our calculations will yield the AsV when ω_0 is known perfectly, which is a lower bound to the AsV of (19). We will begin with the case where the samples $x[n]$ are independent. Let $d(N) = \sqrt{N}$, $g(a_1, a_2) = |a_1|^2/(a_2 - |a_1|^2)$ (c.f. (19)), $x_1 = Ae^{j\phi_0}$ and $x_2 = \Omega$ (because (17) converges to $Ae^{j\phi_0}$ and (18) converges to Ω). To calculate the c_{lk} in (11) we will use the following covariance expressions which are straightforward to show [23]:

$$\mathrm{var}(X_1(N)) = \sigma^2 \frac{1}{N} \sum_{k=-N+1}^{N-1} \left(1 - \frac{|k|}{N}\right) r_h[k]\, e^{-j\omega_0 k}\,, \tag{20}$$

$$\mathrm{var}(X_2(N)) = \frac{\Omega^2}{(K+1)^2} \frac{1}{N} \sum_{k=-N+1}^{N-1} \left(1 - \frac{|k|}{N}\right) \left[|r_h[k]|^2 + 2K\mathrm{Re}\left(r_h[k]\, e^{-j\omega_0 k}\right)\right]\,, \tag{21}$$

$$\mathrm{cov}(X_1(N), X_2(N)) = Ae^{j\phi_0}\sigma^2 \frac{1}{N} \sum_{k=-N+1}^{N-1} \left(1 - \frac{|k|}{N}\right) r_h[k]\, e^{j\omega_0 k}\,. \tag{22}$$

where $r_h[k] := r_h(kT_s)$, and $\mathrm{Re}(\cdot)$ denotes real part. Using (20)-(22) with $r_h[k] = \delta[k]$ [2], we obtain $c_{11} = \sigma^2$, $c_{12} = c_{21}^* = Ae^{j\phi_0}\sigma^2$, and $c_{22} = \Omega^2(2K+1)/(K+1)^2$. Differentiating $g(a_1, a_2)$ we get $\partial g(a_1, a_2)/\partial a_1 = Ae^{-j\phi_0}\Omega/\sigma^2$, $\partial g(a_1, a_2)/\partial a_2 = -A^2/\sigma^4$ and substituting in (12), and simplifying, we finally obtain

$$\mathrm{AsV}(\hat{K}_{\mathrm{IQ}}) = K(K^2 + K + 1)\,. \tag{23}$$

We observe that this simple polynomial function of K suggests that the estimator should be more accurate for smaller values of K. This is observed in Fig. 4 where we compare (13) with (23), and observe that until $K = 3$, the I/Q estimator has a better asymptotic performance.

The more realistic, but challenging problem is calculating the asymptotic variance when the samples $x[n]$ are correlated. If the correlations of $x[n]$ are well-behaved enough for $\sum_k |r_h[k]| < \infty$ to hold (as seen in exponentially-decaying ARMA, or Gaussian shaped correlation functions) then (20)-(22) are $\mathcal{O}(N^{-1})$, so the rate of convergence is the same as the iid case [3]. We will, however, adopt the model in (2) for the correlation function, which is *not* absolutely summable, but has the merits of being motivated by physical considerations. Moreover, (2) does not constrain our results to isotropic scattering, i.e, $p_h(\theta)$ does not have to be equal to $1/(2\pi)$ in $-\pi \le \theta < \pi$, which allows for directional receptions, and generalizes Clarke-Jakes model [19]. To our knowledge, this is the first time that (2) is used in performance analysis of estimators in wireless communications.

[2] Krönecker's delta function $\delta[k]$ is used because the samples are assumed uncorrelated.

[3] We will use the standard notation $F(N) = \mathcal{O}(G(N))$ to mean that $F(N)/G(N)$ is a bounded sequence.

Let us first characterize the asymptotic behavior of $r_h(\tau)$, which will be central in the calculation of the asymptotic variance. Using the method of stationary phase, it can be shown that (2) can be expressed as [4]:

$$r_h(\tau) = (f_D\tau)^{-1/2}\left[p_h(0)\, e^{j(2\pi f_D\tau - \frac{\pi}{4})} + p_h(\pi)\, e^{-j(2\pi f_D\tau - \frac{\pi}{4})}\right] + \mathcal{O}(\tau^{-1})\,. \tag{24}$$

Notice that when $p_h(\theta)$ is uniform, $r_h(\tau) \sim (f_D\tau)^{-1/2}\cos(2\pi f_D\tau - \pi/4)$, which is a well-known asymptotic expansion of $J_0(\cdot)$. Hence, we reach the interesting conclusion that under some regularity conditions on $p_h(\theta)$, for large enough τ, the correlation function is the sum of a sinusoid whose envelope goes to zero as $\tau^{-1/2}$ and an error term which goes to zero faster as τ^{-1}. In our AsV derivation for $\hat{K}_{\rm IQ}$ in (19), we will need the correlation function for the *sampled* I/Q components. Recalling that $\omega_D = 2\pi f_D T_s$, the sampled correlation function can be expressed, using (24) as

$$r_h[k] = \left(\frac{2\pi}{\omega_D k}\right)^{1/2}\left[p_h(0)\, e^{j(\omega_D k - \frac{\pi}{4})} + p_h(\pi)\, e^{-j(\omega_D k - \frac{\pi}{4})}\right] + \mathcal{O}(k^{-1})\,. \tag{25}$$

Notice that the correlation in (25) are not absolutely summable. The slow-decaying nature of the correlation function in (25) results in a slower convergence rate for $X_1(N)$ and $X_2(N)$ as compared to the independent case. First let us determine how fast the variances of $X_1(N)$ and $X_2(N)$ in (17) and (18) go to zero. We will then invoke the Theorem in Section II to determine the rate of convergence of $\hat{K}_{\rm IQ}(N)$ which is the goal in this subsection.

Using (25) and (20) we show in Appendix III the following: [4]

$$\mathrm{var}(X_1(N)) = \begin{cases} \mathcal{O}(N^{-1}) & \text{if } |\omega_0| < \omega_D \\ \mathcal{O}(N^{-\frac{1}{2}}) & \text{if } |\omega_0| = \omega_D \end{cases}\,, \tag{26}$$

and similarly, using (25) and (21), we show in Appendix III that

$$\mathrm{var}(X_2(N)) = \begin{cases} \mathcal{O}(N^{-1}\log(N)) & \text{if } |\omega_0| < \omega_D \\ \mathcal{O}(N^{-\frac{1}{2}}) & \text{if } |\omega_0| = \omega_D \end{cases}\,. \tag{27}$$

Comparing (20) and (22), it is apparent that $\mathrm{var}(X_1(N))$ and $\mathrm{cov}(X_1(N), X_2(N))$ converge at the same rate given by (26).

Recall that when the samples are independent (or more generally when $\sum_k |r_h[k]| < \infty$), the convergence rate of the variances of both $X_1(N)$ and $X_2(N)$ is $d^{-2}(N) = N^{-1}$. It is interesting that, for correlation functions of the form in (2), the rate of convergence of both $X_1(N)$ and $X_2(N)$ depends on whether $|\omega_0| = \omega_D$. Physically, $|\omega_0| = \omega_D$ when $\theta_0 = 0$ in (1), i.e., the LoS is in the

[4]Notice that since $\omega_0 = \omega_D\cos(\theta_0)$, $|\omega_0| \le \omega_D$ always holds, so we do not consider the case $\omega_0 > \omega_D$.

same direction as the mobile. So, when $|\omega_0| < \omega_D$, $X_1(N)$ converges faster than $X_2(N)$, and when $|\omega_0| = \omega_D$, the variances of $X_1(N)$ and $X_2(N)$ converge to zero at the same rate. Now we are ready to invoke the Theorem of Section II.

The Theorem requires that both $X_1(N)$ and $X_2(N)$ should converge when scaled by the same sequence. So, when $|\omega_0| < \omega_D$, the scaling sequence should be the slower of the $X_1(N)$ and $X_2(N)$, so that the faster one will converge to zero (if we were to scale with the rate of the faster one, the slower statistic would go to infinity). Hence, when $|\omega_0| < \omega_D$, we choose $d(N)$ so that $d^{-2}(N) = N^{-1}\log(N)$. To calculate the AsV, we need to substitute in (12), $d(N) = \sqrt{N/\log(N)}$, the partial derivatives of $g(a_1, a_2)$, which are given right before (23), and c_{lk} which, using (11), (20)-(22), (26) and (27), are given by $c_{11} = c_{12} = c_{21} = 0$, and $c_{22} = [\Omega^2/(K+1)^2]\, C_1$, where C_1 and the resulting AsV are given by

$$\mathrm{AsV}(\hat{K}_{\mathrm{IQ}}) = K^2 \underbrace{\left[\lim_{N\to\infty} \frac{1}{\log(N)} \sum_{k=-N+1}^{N-1} \left(1 - \frac{|k|}{N}\right) |r_h[k]|^2\right]}_{=:C_1}, \quad |\omega_0| < \omega_D \,, \tag{28}$$

and the limit C_1, which is independent of K, can be shown to exist using (25). When $|\omega_0| = \omega_D$ we have that both $X_1(N)$ and $X_2(N)$ converge at the same rate. So we select $d^{-2}(N) = N^{-1/2}$ and substitute in (12) $d(N) = \sqrt{N^{1/2}}$, the partial derivatives, and c_{lk}, which, using (11) and (20-27) turn out to be $c_{11} = \Omega C_2$, $c_{12} = c_{21}^* = Ae^{j\phi_0}\sigma^2 C_2$, and $c_{22} = \Omega^2 2K/(K+1)^2\, C_2$, where C_2 and the resulting AsV are given by

$$\mathrm{AsV}(\hat{K}_{\mathrm{IQ}}) = (K^3 + K) \underbrace{\left[\lim_{N\to\infty} N^{-1/2} \sum_{k=-N+1}^{N-1} \left(1 - \frac{|k|}{N}\right) r_h[k]\, e^{j\omega_0 k}\right]}_{=:C_2}, \quad |\omega_0| = \omega_D \tag{29}$$

and the limit C_2 is independent of K.

Hence, loosely speaking, we can say that when the data are independent the AsV of $\hat{K}_{\mathrm{IQ}}(N)$ is proportional to $K(K^2 + K + 1)$ when the estimator is scaled by $d(N) = \sqrt{N}$; when the data are correlated with correlation function given in (2), we have the case $|\omega_0| < \omega_D$: the AsV of $\hat{K}_{\mathrm{IQ}}(N)$ is proportional to K^2 when the estimator is scaled by $d(N) = \sqrt{N/\log(N)}$; and the case $|\omega_0| = \omega_D$: the AsV of $\hat{K}_{\mathrm{IQ}}(N)$ is proportional to $K^3 + K$ when the estimator is scaled by $d(N) = \sqrt{N^{1/2}}$.

Some conclusions that we can draw from this analysis are as follows. Regardless of whether the data samples are correlated or not, the $\hat{K}_{\mathrm{IQ}}$ becomes more accurate if K is small. In fact, our motivation for pursuing the estimation of K from the I/Q components was precisely this reason: while all unbiased estimators of K from the envelope yield an unbounded variance as K gets smaller, the accuracy of $\hat{K}_{\mathrm{IQ}}$ increases with smaller K. It is also important to notice that the value of ω_0 makes

a difference in the performance, so much so that it makes a difference in the *rate* of convergence. In fact even for finite N, motivated by Remark 1 following (16), values of ω_0 for which $S_h(\omega_0)$ is small, yield better performance. If we adopt the isotropic scattering model, corresponding to a uniform $p_h(\theta)$, $S_h(\omega) = \sigma_h^2 \pi^{-1}[1-(\omega/\omega_D)^2]^{-1/2}, |\omega| < \omega_D$. Since $S_h(\omega_D)$ is infinite, when $|\omega_0| = \omega_D$ the performance is worse as compared to when $|\omega_0| < \omega_D$. This spectrum has a minimum at 0, hence, $\omega_0 = 0$ (implying $\theta_0 = \pi/2$) seems to be the best AoA for the LoS component as far as the performance of $\hat{K}_{\mathrm{IQ}}$ is concerned. Physically, this is a LoS that is perpendicular to the direction of the mobile yielding a time-invariant LoS component.

IV. Simulations

In this section we provide a computer simulation study of the various estimators. The signal from which the K factor is estimated has been generated using a sum of sinusoids model the details of which can be found in [23].

A. Envelope-Based Estimators: Comparison with the MLE and Effect of Finite Sample Size

The MLE of K for the envelope data is given in (8) and is known to be very close to the CRB for large number of data samples. Since $\hat{K}_{1,2}$ is also very close to the CRB, as evidenced by Fig. 2, we know that the moment-based estimators perform similar to the MLE for large N. In order to answer the question of how the moment-based estimators compare with the MLE for *finite* data samples, we show the performance of $\hat{K}_{1,2}$ along with the MLE in Fig. 5 for $N = 100$. The MLE was calculating using an exhaustive search for the value of K that satisfies (**??**). We observe that even for small values of N, the MLE is only slightly better than the simpler moment-based estimator. The same trend was observed even when the envelope samples were correlated (not shown). We have also plotted the envelope CRB in Fig. 5 for reference. We observe that for small values of K, the estimation errors [5] of $\hat{K}_{1,2}$ and the MLE are better than the CRB. This can only be explained by the fact that the CRB is a lower bound on the variance of *unbiased* estimators and that the MLE and $\hat{K}_{1,2}$ are biased for finite data samples. It is well-known that the CRB need not be a lower bound on the estimation error of biased estimators [17]. However, the envelope CRB seems to be a useful benchmark for moderate values of K. We will now elaborate more on the effect of finite sample size, comparing the different moment-based estimators.

In order to study the effect of finite sample size on the performance of $\hat{K}_{1,2}$ and $\hat{K}_{2,4}$, we resorted to Monte Carlo simulations. For any fixed K from the set $\{0.5, 1, 1.5, \ldots, 19.5, 20\}$, broad enough to cover a practical range of the K parameter [7], and for any $N \in \{100, 1000\}$, 500 sequences

[5] the estimation error is defined to be the variance plus the square of the bias so that the error in bias is also reflected in Fig. 5

of i.i.d. samples of length N were generated for calculating $\hat{K}_{1,2}$ and $\hat{K}_{2,4}$. Let $\hat{K}(j)$ denote the j^{th} Monte Carlo realization of either $\hat{K}_{1,2}$ or $\hat{K}_{2,4}$. For both of these estimators the sample bias $500^{-1}\sum_{j=1}^{500}[\hat{K}(j) - K]$ is plotted in Fig. 6 versus K, together with the sample confidence region defined by ± 2 SSTD($\hat{K}$), where SSTD($\hat{K}$) is the sample standard deviation of $\hat{K}$, defined as:

$$\mathrm{SSTD}(\hat{K}) := \sqrt{500^{-1}\sum_{j=1}^{500}\hat{K}^2(j) - (500^{-1}\sum_{j=1}^{500}\hat{K}(j))^2}\ .$$

The sample confidence region defined here is useful for examining the estimator variations in terms of K and N.

The top four plots in Fig. 6 show that the confidence region and the sample bias are smaller for larger sample sizes. We also observe that for moderate/large K, increasing K increases the bias especially for $N = 100$, for both $\hat{K}_{1,2}$ and $\hat{K}_{2,4}$. The bottom two plots of Fig. 6 illustrate that the estimation error of $\hat{K}_{1,2}$ and $\hat{K}_{2,4}$ are very similar and close to the envelope CRB for both sample sizes.

B. Envelope-Based Estimators: Effect of Correlation

In practice, adjacent signal samples can be highly correlated. To analyze the impact of correlated samples on the performance of $\hat{K}_{1,2}$ and $\hat{K}_{2,4}$, we used Monte Carlo simulations. Using the same simulation procedure as before and for $N = 1,000$, we generated 500 Rice distributed envelope time-series whose corresponding in-phase and quadrature components have the Clarke's correlation function. Fig. 7 shows the simulation results for two different mobile speeds (different f_Ds), at a sampling rate of $1/T_s = 243$ Hz, corresponding to samples taken from an IS-136 system every 100 symbols. For both estimators, the correlation among samples, which increases with decreasing mobile speed, introduces a positive bias which grows with K and also broadens the sample confidence region (more estimator variation). Based on the simulation results, we conclude that $\hat{K}_{1,2}$ and $\hat{K}_{2,4}$ still perform close to each other even for correlated samples, and that the samples should be chosen far apart to avoid the deleterious effects of correlation on the estimates. To illustrate the performance degradation due to correlation as compared to the performance with independent samples, the last two plots of Fig. 7 show the estimation error of $\hat{K}_{1,2}$ and $\hat{K}_{2,4}$ for correlated samples with the envelope CRB for the uncorrelated case.

C. Comparison of Envelope and I/Q estimators of K

To test the possible improvements attainable by using the I/Q components in estimating K as compared to envelope-based estimators, we compared the I/Q estimator of Section III, with the

envelope-based $\hat{K}_{1,2}$. We chose $N = 1,000$ data points, and $\omega_D = 18.85$ which corresponds to a vehicle velocity of $v = 100$ km/hr, $T_s = 0.01$ sec., and a carrier frequency of 900 MHz. We observe from Fig. 8 that the estimator that relies on the I/Q components performs significantly better than $\hat{K}_{1,2}$. Moreover, the I/Q CRB provides a tight lower bound on the estimation error of the I/Q estimator particularly for small values of K. This is at the expense of a slight increase in computational complexity, and the necessity of measuring the I/Q components of the received signal.

V. Conclusions

We started out by proposing a new family of estimators for K from the envelope samples. This general class of estimators was shown to unify the existing approaches in the literature. We derived the asymptotic variance of each member of this family of moment-based estimators and showed that they perform close to the CRB. Two moment-based estimators $\hat{K}_{1,2}$ and $\hat{K}_{2,4}$ were worthy of special attention because $\hat{K}_{1,2}$ had the best asymptotic performance, and $\hat{K}_{2,4}$ had a simple closed-form expression in terms of the moments. It was mentioned that a real-time low-complexity implementation of these estimators should use a sliding window approach to estimating the necessary moments.

Motivated by the fact that the envelope CRB increases without bound as K gets smaller, we studied the estimation of K from the I/Q data. We observed that the I/Q CRB goes to zero as K gets smaller, a property also held by the AsV of a novel I/Q-based estimator that we proposed. The performance analysis for this estimator for correlated samples yielded insights into the effect of θ_0 on the estimator performance. The simulations corroborate the analytical findings of the previous sections and illustrate that the moment-based estimators that use the envelope are very close to the MLE even for finite sample sizes, and that $\hat{K}_{\mathrm{IQ}}$ outperforms $\hat{K}_{1,2}$.

We conclude that among the moment-based estimators from the envelope $\hat{K}_{2,4}$ is computationally simpler than $\hat{K}_{1,2}$, at the expense of a loss in performance. We also suggest that the I/Q components be used when they are available for estimation of K because they offer an improvement in performance over the envelope-based estimators.

Acknowledgement: The authors would like to thank Prof. Mostafa Kaveh of the University of Minnesota for his valuable comments and insight.

Appendix I: *CRB for Envelope-Based Estimators*

It is straightforward to show the following:

$$\frac{\partial \ln(p_R(r))}{\partial K} = \frac{1}{K+1} - 1 - \frac{r^2}{\Omega} + \frac{I_1\left(2r\sqrt{\frac{K(K+1)}{\Omega}}\right)}{I_0\left(2r\sqrt{\frac{K(K+1)}{\Omega}}\right)} \frac{2K+1}{\sqrt{\Omega K(K+1)}} r \tag{30}$$

$$\frac{\partial \ln(p_R(r))}{\partial \Omega} = -\frac{1}{\Omega} + \frac{(K+1)r^2}{\Omega^2} - \frac{I_1\left(2r\sqrt{\frac{K(K+1)}{\Omega}}\right)}{I_0\left(2r\sqrt{\frac{K(K+1)}{\Omega}}\right)} \sqrt{\frac{K(K+1)}{\Omega^3}} r \ . \tag{31}$$

Let $[\mathbf{M}]_{kl}$ denote the (k,l) entry of a generic matrix $\mathbf{M}$. Defining the FIM entries as

$$\begin{aligned}
[\mathbf{J}(K)]_{11} &= N \int_0^\infty \left(\frac{\partial \ln p_R(r)}{\partial K}\right)^2 p_R(r)\, dr \\
[\mathbf{J}(K)]_{12} &= N \int_0^\infty \frac{\partial \ln p_R(r)}{\partial K} \frac{\partial \ln p_R(r)}{\partial \Omega} p_R(r)\, dr \\
[\mathbf{J}(K)]_{21} &= N\, [\mathbf{J}(K)]_{12} \\
[\mathbf{J}(K)]_{22} &= N \int_0^\infty \left(\frac{\partial \ln p_R(r)}{\partial \Omega}\right)^2 p_R(r)\, dr \ ,
\end{aligned}$$

we can express the CRB for the envelope data for unknown Ω as the (1,1) element of the inverse FIM, which is easily shown to be:

$$\mathrm{CRB}(K) = \frac{[\mathbf{J}(K)]_{22}}{N([\mathbf{J}(K)]_{11}\,[\mathbf{J}(K)]_{22} - [\mathbf{J}(K)]_{21}^2)} \ . \tag{32}$$

Notice that the entries of the FIM need to be computed with numerical integration using (31). Notice also that (14) is given by $1/[\mathbf{J}(K)]_{11}$, and is smaller than or equal to (32) because $[\mathbf{J}(K)]_{21}^2 \geq 0$ in (32).

Appendix II:*CRB for I/Q - Based Estimators*

For I/Q data which is complex Gaussian with mean $\mathbf{m}(\boldsymbol{\zeta})$ and covariance matrix $\boldsymbol{\Gamma}(\boldsymbol{\zeta})$, the elements of the FIM are given by [26]

$$[\mathbf{J}(\boldsymbol{\zeta})]_{kl} = 2\mathrm{Re}\left[\left(\frac{\partial \mathbf{m}(\boldsymbol{\zeta})}{\partial \zeta_k}\right)^H \boldsymbol{\Gamma}^{-1}(\boldsymbol{\zeta}) \left(\frac{\partial \mathbf{m}(\boldsymbol{\zeta})}{\partial \zeta_l}\right)\right] + \mathrm{tr}\left[\boldsymbol{\Gamma}^{-1}(\boldsymbol{\zeta}) \frac{\partial \boldsymbol{\Gamma}(\boldsymbol{\zeta})}{\partial \zeta_k} \boldsymbol{\Gamma}^{-1}(\boldsymbol{\zeta}) \frac{\partial \boldsymbol{\Gamma}(\boldsymbol{\zeta})}{\partial \zeta_l}\right] \ , \tag{33}$$

where ζ_k denotes the k^{th} element of $\boldsymbol{\zeta}$, and $\mathrm{tr}(\cdot)$ denotes the trace of a matrix.

We now calculate the CRB for estimators of K that use the I/Q components assuming that all the elements in $\boldsymbol{\zeta}$ are unknown. For this, we need the partial derivatives of $\mathbf{m}(\boldsymbol{\zeta})$ and $\boldsymbol{\Gamma}(\boldsymbol{\zeta})$ with respect to ζ_k, which are given below:

$$\begin{aligned}
&\frac{\partial \mathbf{m}(\boldsymbol{\zeta})}{\partial K} = \frac{\sigma}{2\sqrt{K}}\mathbf{e}(\omega_0,\phi_0) && \frac{\partial \mathbf{m}(\boldsymbol{\zeta})}{\partial \sigma} = \sqrt{K}\mathbf{e}(\omega_0,\phi_0)\\
&\frac{\partial \mathbf{m}(\boldsymbol{\zeta})}{\partial \omega_0} = \sigma\sqrt{K}e^{j(\phi_0+\pi/2)}[0e^{j\omega_0 0}\ldots(N-1)e^{j\omega_0(N-1)}]^T && \frac{\partial \mathbf{m}(\boldsymbol{\zeta})}{\partial \phi_0} = j\sqrt{K}\sigma\mathbf{e}(\omega_0,\phi_0)\\
&\frac{\partial \boldsymbol{\Gamma}(\boldsymbol{\zeta})}{\partial \sigma} = 2\sigma\mathbf{R}(\omega_D) && \frac{\partial \boldsymbol{\Gamma}(\boldsymbol{\zeta})}{\partial \omega_D} = \sigma^2\mathbf{R}'(\omega_D)\\
&\frac{\partial \mathbf{m}(\boldsymbol{\zeta})}{\partial \omega_D} = \frac{\partial \boldsymbol{\Gamma}(\boldsymbol{\zeta})}{\partial K} = \frac{\partial \boldsymbol{\Gamma}(\boldsymbol{\zeta})}{\partial \omega_0} = \frac{\partial \boldsymbol{\Gamma}(\boldsymbol{\zeta})}{\partial \phi_0} = \mathbf{0}
\end{aligned} \tag{34}$$

where $[\mathbf{R}'(\omega_D)]_{kl} = \partial J_0(\omega_D(k-l))/\partial\omega_D = -(k-l)J_1(\omega_D(k-l))$. Using (34) and (33), all entries of the 5×5 FIM can be computed, and the (1,1) element of the inverse FIM will be the CRB of K estimators that utilize the I/Q components when $\boldsymbol{\zeta}$ is unknown. Let $J_{11} := [\mathbf{J}(\boldsymbol{\zeta})]_{11}$ for brevity. An important point is that J_{11} is proportional to $1/K$ and hence goes to infinity as K goes to zero. Also the submatrix $[\mathbf{J}(\boldsymbol{\zeta})]_{2:5,2:5}$ consisting of the second through fifth row, and second through fifth column of $[\mathbf{J}(\boldsymbol{\zeta})]$, stays constant as K goes to zero. This can be easily verified using (34) and (33). Furthermore, let $[\mathbf{J}(\boldsymbol{\zeta})]_{1,2:5}$ and $[\mathbf{J}(\boldsymbol{\zeta})]_{2:5,1}$ be vectors consisting of the second through fifth column of the first row and second through fifth row of the first column, respectively. Then, as a consequence of the matrix inversion lemma [16, pp. 512], the (1,1) element of the inverse FIM (which is the CRB of interest) is given by

$$[\mathbf{J}^{-1}(\boldsymbol{\zeta})]_{11} = \frac{1}{J_{11}} + [\mathbf{J}(\boldsymbol{\zeta})]_{1,2:5}\left(J_{11}^2[\mathbf{J}(\boldsymbol{\zeta})]_{2:5,2:5} - J_{11}[\mathbf{J}(\boldsymbol{\zeta})]_{2:5,1}[\mathbf{J}(\boldsymbol{\zeta})]_{1,2:5}\right)^{-1}[\mathbf{J}(\boldsymbol{\zeta})]_{2:5,1}. \tag{35}$$

But as K goes to zero, J_{11} goes to infinity, and all the other terms remain bounded, which shows that $[\mathbf{J}^{-1}(\boldsymbol{\zeta})]_{11}$ in (35), which is the CRB of interest, goes to zero as K goes to zero.

Appendix III:*Rates of Convergence*

In this appendix, we will derive (26) and (27). In order to show (26) for $|\omega_0| < \omega_D$, we need to show that $N\mathrm{var}(X_1(N))$ converges to a finite constant. To show that $N\mathrm{var}(X_1(N))$ converges, we need to establish $\sum_{k=-\infty}^{\infty}(1-|k|/N)r_h[k]e^{-j\omega_0 k} < \infty$ for which it suffices to show that $\sum_{k=-\infty}^{\infty} r_h[k]e^{-j\omega_0 k} < \infty$ because of the Cesaro summability theorem [13, pp. 411]. Substituting (25) for $r_h[k]$ we can write $r_h[k]e^{-j\omega_0 k} \approx a[k]b[k]$ where

$$b[k] := p_h(0)\, e^{j((\omega_D-\omega_0)k-\frac{\pi}{4})} + p_h(\pi)\, e^{-j((\omega_D+\omega_0)k-\frac{\pi}{4})},\quad a[k] := \left(\frac{2\pi}{\omega_D k}\right)^{1/2}, \tag{36}$$

and the approximation is due to the $\mathcal{O}(k^{-1})$ term in (25). We can now apply Drichlet's test [2, pp. 365] which states that if $a[k]$ converges monotonically to zero and the partial sums of $b[k]$ are bounded, then $\sum_k a[k]b[k]$ converges. Since these two conditions hold in our case ($|\omega_0| < \omega_D$), we conclude that $\sum_{k=-\infty}^{\infty} r_h[k]e^{-j\omega_0 k} < \infty$, which is what we needed to show.

Let us now show that (26) for $|\omega_0| = \omega_D$ holds. To do this, we need to show that

$$\sum_{k=-N+1}^{N-1} \left(1 - \frac{|k|}{N}\right) r_h[k]e^{-j\omega_D k} \approx \sum_{k=-N+1}^{N-1} \left(1 - \frac{|k|}{N}\right) a[k]\ b[k] = \mathcal{O}(N^{1/2}). \tag{37}$$

where $a[k]$ and $b[k]$ are obtained by substituting $|\omega_0| = \omega_D$ in (36) and are given by $a[k] = [(2\pi)/(\omega_D k)]^{1/2}$, $b[k] = [p_h(0)\ \exp(-j\frac{\pi}{4}) + p_h(\pi)\ \exp -j((\omega_D + \omega_0)k - \frac{\pi}{4})]$, which is the sum of a constant and an exponential. But $\sum_{k=-N+1}^{N-1} a[k]b[k]$ and $N^{-1}\sum_{k=-N+1}^{N-1} |k|a[k]b[k]$ add up to (37), and they are both $\mathcal{O}(N^{1/2})$. This can be seen after substituting for $a[k]$ and $b[k]$, and using the following: [6] $\sum_{k=-N+1}^{N-1} k^{-1/2} = \mathcal{O}(N^{1/2})$, $N^{-1}\sum_{k=-N+1}^{N-1} k^{1/2} = \mathcal{O}(N^{1/2})$, and $\sum_{k=-N+1}^{N-1} k^{-1/2}$ $e^{-j((\omega_D+\omega_0)k-\frac{\pi}{4})} = \mathcal{O}(1)$, where the first two equalities are obtained by integrating $k^{-1/2}$ and $k^{1/2}$ respectively, and the third expression is obtained using Drichlet's theorem. This establishes the equality in (37) which is what we wanted to show.

We will now show that (27) holds. For $|\omega_0| < \omega_D$, we need to show that

$$\sum_{k=-N+1}^{N-1} \left(1 - \frac{|k|}{N}\right) \left[|r_h[k]|^2 + 2K\mathrm{Re}\left(r_h[k]e^{-j\omega_0 k}\right)\right] = \mathcal{O}(\log(N))\ , \tag{38}$$

which would establish that (21) is $\mathcal{O}(N^{-1}\log(N))$. We know from (26) that for $|\omega_0| < \omega_D$, $\sum_k r_h[k]e^{j\omega_0 k}$ converges; hence, we can do away with the second term in the square brackets in (38), and see that establishing (38) amounts to showing

$$\sum_{k=-N+1}^{N-1} |r_h[k]|^2 - \sum_{k=-N+1}^{N-1} \frac{|k|}{N}|r_h[k]|^2 = \mathcal{O}(\log(N))\ . \tag{39}$$

Using (25), it is straightforward to show that the first term on the left hand side of (39) is

$$\sum_{k=-N+1}^{N-1} |r_h[k]|^2 \approx \left(\frac{2\pi}{\omega_D}\right) \sum_{k=-N+1}^{N-1} \left(\frac{p_h^2(0) + p_h^2(\pi)}{k} + 2p_h(0)p_h(\pi)\frac{\cos\left(\omega_D k - \frac{\pi}{4}\right)}{k}\right)\ , \tag{40}$$

which is $\mathcal{O}(\log(N)) + \mathcal{O}(1)$, where the $\mathcal{O}(\log(N))$ term is obtained by integrating k^{-1}, and the $\mathcal{O}(1)$ term is obtained by using Drichlet's theorem. But the second term on the left hand side of

[6] Since we are interested in asymptotic expressions for large N, we are not concerned with the fact that $k^{-1/2}$ is unbounded for $k = 0$

(39) is $\sum_{k=-N+1}^{N-1}(|k|/N)|r_h[k]|^2 = \mathcal{O}(1)$, which can be verified similar to (40). So (39) must be $\mathcal{O}(\log(N))$. This establishes what we wanted to show.

Using a similar approach, it is not difficult to show that for the case $|\omega_0| = \omega_D$, (38) is given by $\mathcal{O}(\log(N)) + \mathcal{O}(N^{1/2}) = \mathcal{O}(N^{1/2})$, which completes the derivations of (26) and (27).

REFERENCES

[1] A. Abdi, C. Tepedelenlioglu, G. B. Giannakis, and M. Kaveh, "On the estimation of the K parameter for the Rice fading distribution," *IEEE Communications Letters*, vol. 5, no. 3, pp. 92-94, 2001.

[2] T. M. Apostol, *Mathematical Analysis*, Addison Wesley, 1957.

[3] S. Catreux, V. Erceg, D. Gesbert, R. W. Heath, "Adaptive modulation and MIMO coding for broadband wireless data networks *IEEE Communications Magazine*, vol. 40, no. 6, June 2002, pp. 108-115.

[4] E. T. Copson, *Asymptotic Expansions*, Cambridge University Press, 1965.

[5] F. Gini, M. Luise and R. Reggiannini, "Cramer-Rao bounds in the parametric estimation of fading radio transmission channels," *IEEE Transactions on Comm.*, vol. 46, no. 10, 1998.

[6] R. Gray, "Toeplitz and circulant matrices: A review," `http://www-ee.stanford.edu/~gray/toeplitz.html`, 2001.

[7] L. J. Greenstein, D. G. Michelson, and V. Erceg, "Moment-method estimation of the Ricean K-factor," *IEEE Communications Letters*, vol. 3, no. 6, pp. 175-176, 1999.

[8] D. Greenwood and L. Hanzo, "Characterization of mobile radio channels," in *Mobile Radio Communications*. R. Steele, Ed., Pentech, 1992, pp. 92-185.

[9] W. K. Hocking, "Reduction of the effects of non-stationarity in studies of amplitude statistics of radio wave backscatter," *Journal of Atmospheric and Terrestrial Physics*, vol. 49, no. 11/12, pp. 1119-1131, 1987.

[10] E. L. Lehmann and G. Casella, *Theory of Point Estimation*, 2nd ed., Springer, 1998.

[11] T. L. Marzetta, "EM algorithm for estimating the parameters of a multivariate complex Ricean density for polarimetric SAR," in *Proc. ICASSP*, Detroit, MI, 1995, pp. 3651-3654.

[12] K. Pahlavan, P. Krishnamurthy, and A. Beneat, "Wideband radio propagation modeling for indoor geolocation applications," *IEEE Communications Magazine*, vol. 36, no. 4, pp. 60-65, 1998.

[13] B. Porat, *Digital Processing of Random Signals*, Prentice Hall, 1994.

[14] F. van der Wijk, A. Kegel, and R. Prasad, "Assessment of a pico-cellular system using propagation measurements at 1.9 GHz for indoor wireless communications," *IEEE Transactions on Vehicular Technology*, vol. 44, no. 1, pp. 155-162, 1995.

[15] P. K. Rastogi and O. Holt, "On detecting reflections in presence of scattering from amplitude statistics with application to *D* region partial reflections," *Radio Science*, vol. 16, no. 6, pp. 1431-1443, 1981.

[16] T. Söderström, and P. Stoica, *System Identification*, Prentice Hall, 1989.

[17] P. Stoica and R. Moses, "On biased estimators and the unbiased CRB," *Signal Processing*, vol. 21, no. 4, pp. 349-350, 1990.

[18] P. Stoica, A. Jakobsson, and J. Li, "Cisoid parameter estimation in the colored noise case: asymptotic Cramer-Rao bound, maximum likelihood, and nonlinear least-squares," *IEEE Trans. on Signal Proc.*, vol. 45, no. 8, pp. 2048-2059, 1997.

[19] G. L. Stüber, *Principles of Mobile Communication*, Kluwer, 1996.

[20] M. Sumanasena, and B. Evans, "Rice factor estimation algorithm," *Electronics Letters*, vol. 37, no. 14, pp. 918-919, 2001.

[21] K. K. Talukdar and W. D. Lawing, "Estimation of the parameters of the Rice distribution," *Journal of Acoustical Society of America*, vol. 89, no. 3, pp. 1193-1197, 1991.

[22] V. Tarokh, N. Seshadri, A. R. Calderbank, "Space-time codes for high data rate wireless communication: performance criterion and code construction," *IEEE Trans. on Info. Theory*, vol. 44, no. 2, March 1998, pp. 744-765.

[23] C. Tepedelenlioğlu and G. B. Giannakis, "On velocity estimation and correlation properties of narrowband communication channels," *IEEE Transactions on Vehicular Technology*, vol. 50, no. 4, pp. 1039-1052, 2001.

[24] C. Tepedelenlioglu, A. Abdi, G. Giannakis, M. Kaveh "Performance Analysis of Moment-Based Estimators for the K Parameter of the Rice Fading Distribution," Proceedings of ICASSP 2001, vol. 4, pp. 2521-2524.

[25] C. Tepedelenlioglu, and A. Abdi, "Estimation of the Rice factor from the I/Q components," *Proc. of the Conference on Information Systems and Sciences*, March 2002.

[26] A. Zeira and A. Nehorai, "Frequency domain Cramer-Rao bound for Gaussian Processes," *IEEE Transactions on Acoustics, Speech, and Signal Processing*, vol 38, no. 6, pp. 1063-1066, 1990.

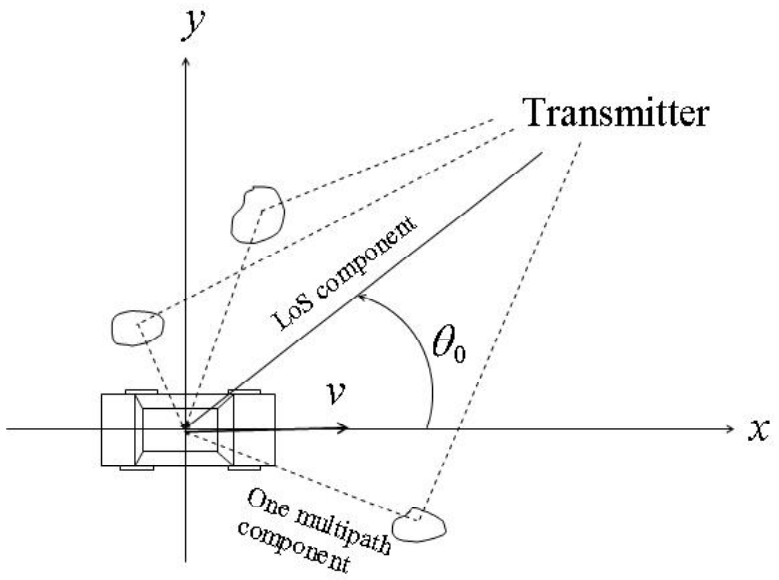

Fig. 1. Multipath propagation environment between transmitter and the mobile receiver

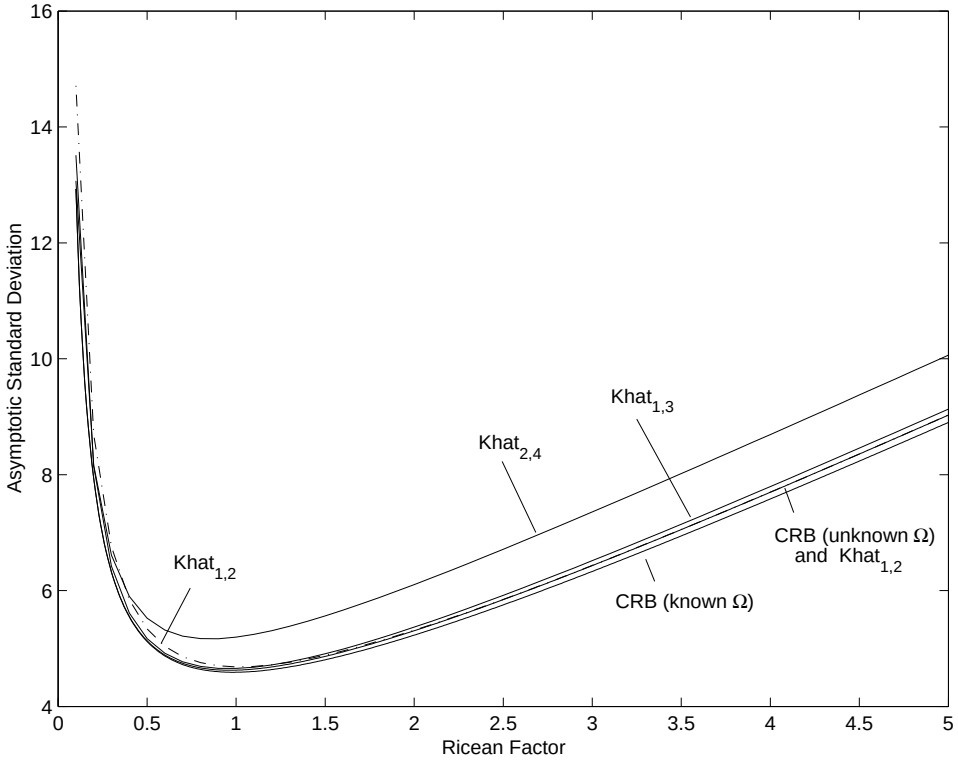

Fig. 2. Asymptotic performance of envelope-based K-estimators and CRB

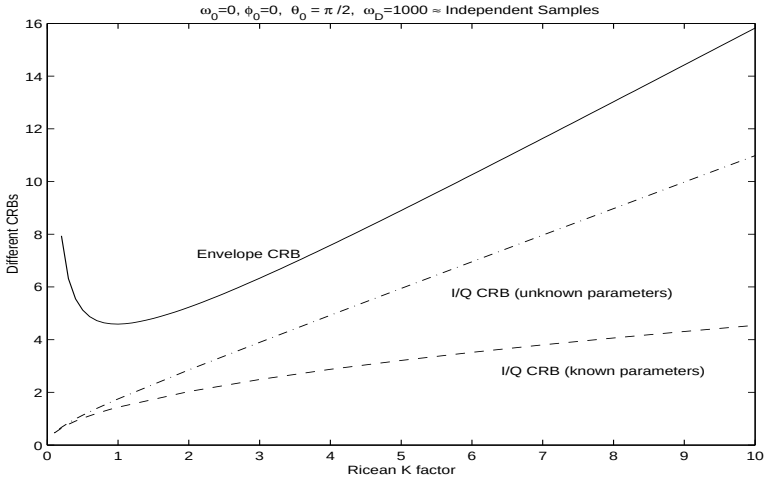

Fig. 3. Different CRBs for K

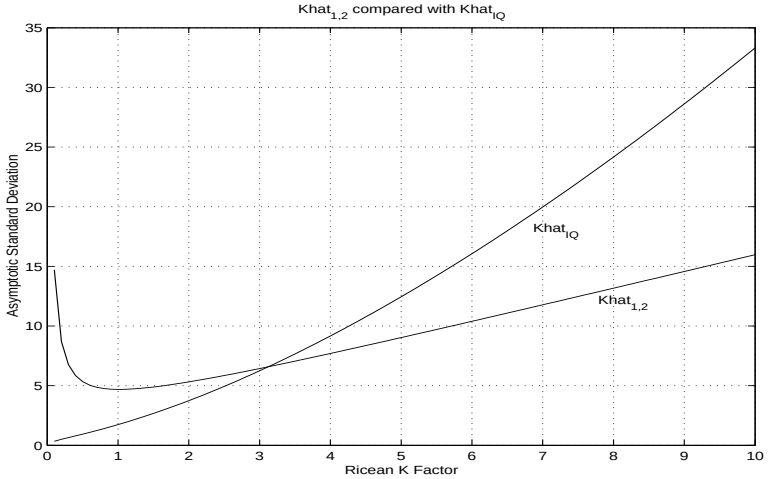

Fig. 4. Comparison of (13) and (23)

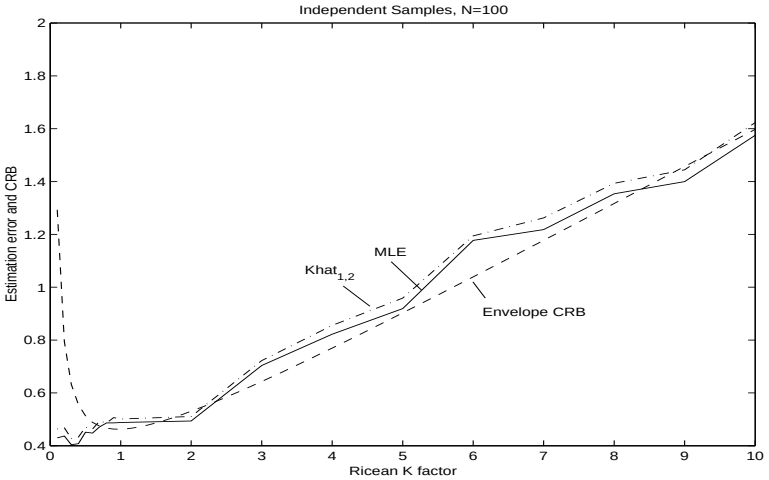

Fig. 5. Comparison of the MLE with $\hat{K}_{1,2}$

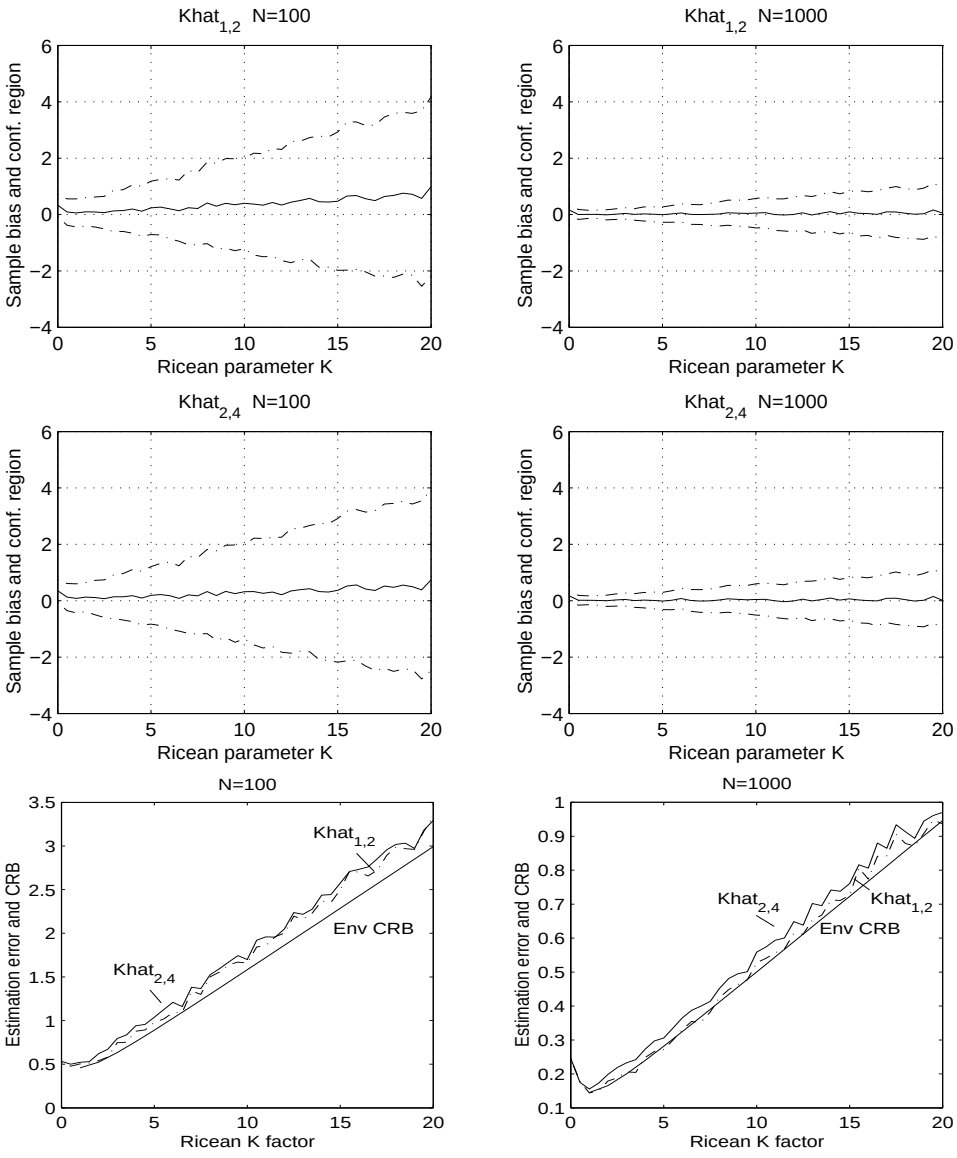

Fig. 6. Monte Carlo simulation for finite sample sizes

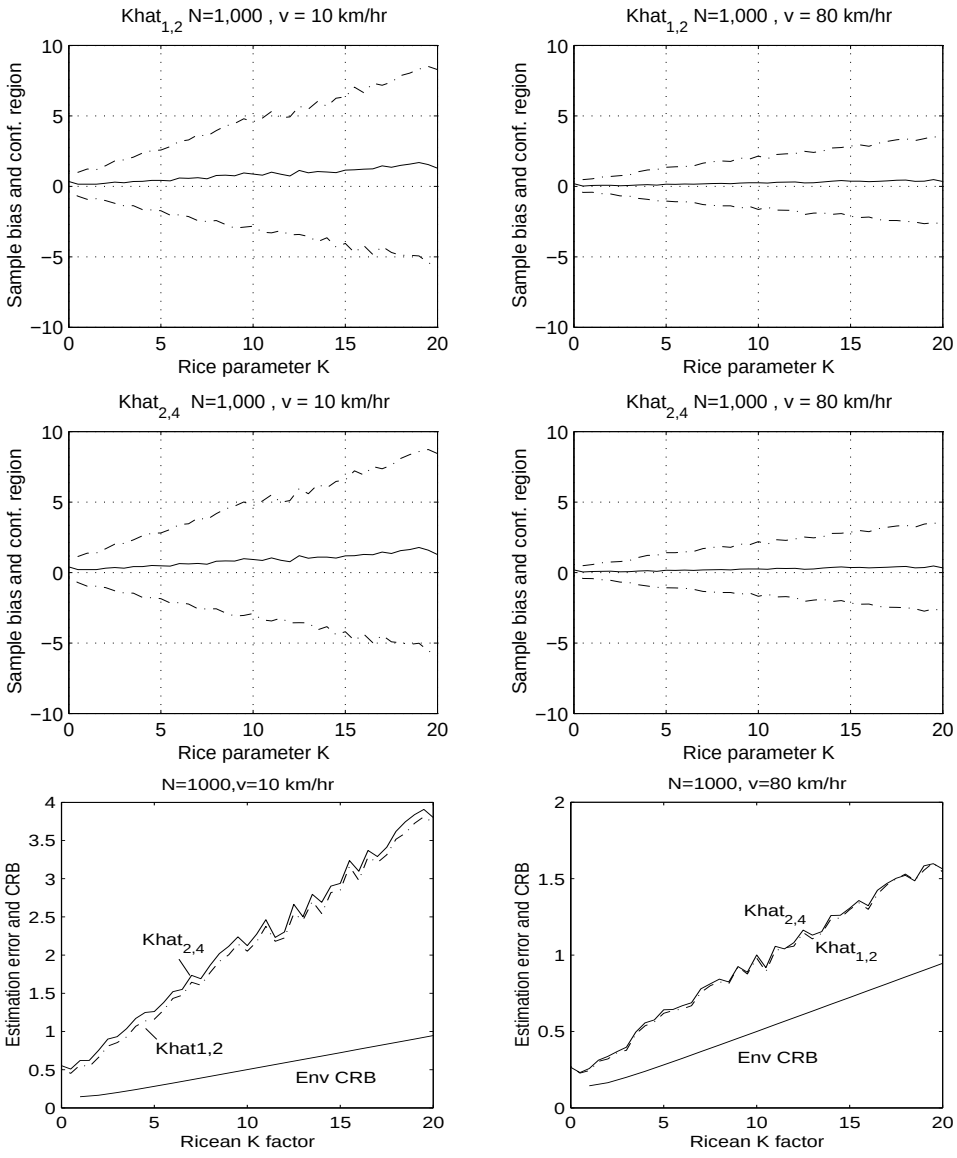

Fig. 7. Monte Carlo simulation for correlated samples

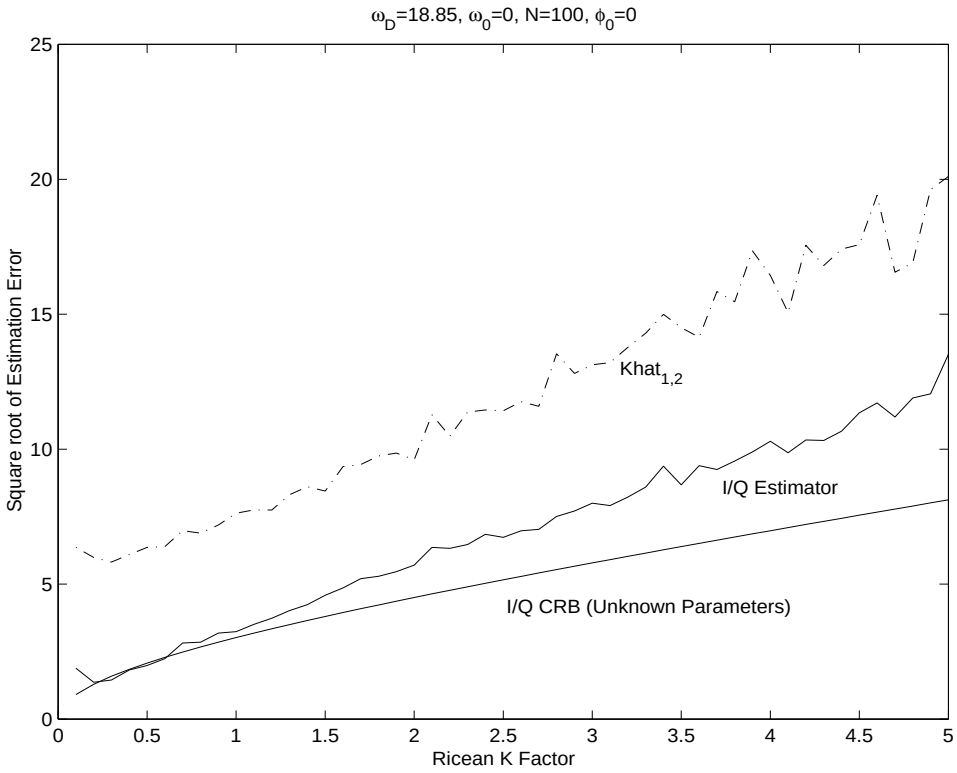

Fig. 8. Comparison of envelope-based and I/Q-based estimators and CRB